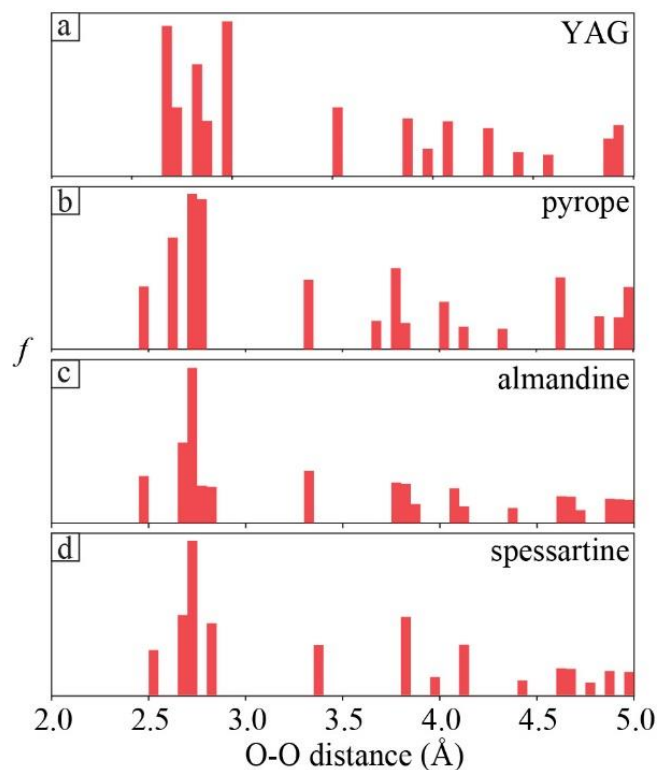


## Appendix 1

### Starting material: crystals

Synthetic undoped YAG ( $\text{Y}_3\text{Al}_5\text{O}_{12}$ ; Table A1-1, see below) was used for most experiments given its stability at high  $T$  (i.e., melting point  $\sim 1970$  °C at 1 atm; Cockayne 1985) and low  $P$  (i.e.,  $< 1$  atm), thus allowing investigation of oxygen diffusivity over a wide range of  $P$ - $T$  conditions. Whilst the composition of YAG probably renders it geologically irrelevant for studying the behavior of cations in garnet, both YAG and pyrope have a cubic  $\text{Ia}\bar{3}\text{d}$  crystal structure. Therefore, we make the first-order assumption that the oxygen sublattice of YAG is a reasonable analogue for natural garnet, which is corroborated by analysis of the inter-oxygen spacing in YAG and pyralspite garnets (Fig. A1-1). Nevertheless, natural crystals of grossular (Grs-2,  $\sim \text{Grs}_{94}\text{Alm}_4\text{Adr}_2$ ; provenance Afghanistan) and pyrope (Prp-1,  $\sim \text{Prp}_{70}\text{Alm}_{30}$ ; provenance Orissa, India) were also used to investigate the effect of chemical composition on oxygen diffusivity.



**Figure A1-1.** Histograms of spacing between oxygen ions in YAG, pyrope, almandine and spessartine derived from X-ray diffraction data, and tabulated by CrystalMakerX software. Bins represent a range of 0.05 Å. Data sources: YAG: Jain et al. (2013); pyrope: Gibbs and Smith (1965); almandine, spessartine: Novak and Gibbs (1971).

---

YAG was analyzed using a CAMECA SX-Five FE electron probe microanalyzer (EPMA) at the Department of Geoscience (University of Wisconsin-Madison, UW-Madison) (Fig. A1-2 and Table A1-1). The composition of YAG starting materials and experimental run products was determined by collection of Y-K $\alpha$  (LPET), Al-K $\alpha$  (LTAP), and O-K $\alpha$  (LPC0) X-rays at both 15 and 7 kV accelerating voltage, 20 nA beam current using a fully focused electron beam (~80 nm diameter; e.g., Moy and Fournelle 2017). Reduction in beam accelerating voltage was used to minimize activation volume for X-ray lines of interest; for example, decreasing from 15 to 7 kV reduces the diameter of activation volume for O-K $\alpha$  from 1400 to 500 nm. Pyrope and grossular crystals were checked for chemical homogeneity with a JEOL JSM-6610A Scanning Electron Microscope (SEM) equipped with an energy-dispersive X-ray analysis (EDXA) system, at the Research School of Earth Sciences (ANU) (Table A1-2, see below). The three garnet starting materials contain variability of less than 1.0 wt.% (2 standard deviation, 2SD) variation in major element composition.

Electron backscattered diffraction (EBSD) analysis was used to investigate the crystallographic orientation and possible decrease in indexation rate of the garnet in the near-interface region in some experimental charges (Fig. A1-3). The mounts were polished with a colloidal silica-based slurry (syton) for 1.5 h prior to EBSD analysis. EBSD maps were collected at 20 kV, 20 nA using an Hitachi S3400 VP-SEM at the Department of Geoscience (UW-Madison) equipped with an Oxford EBSD detector.

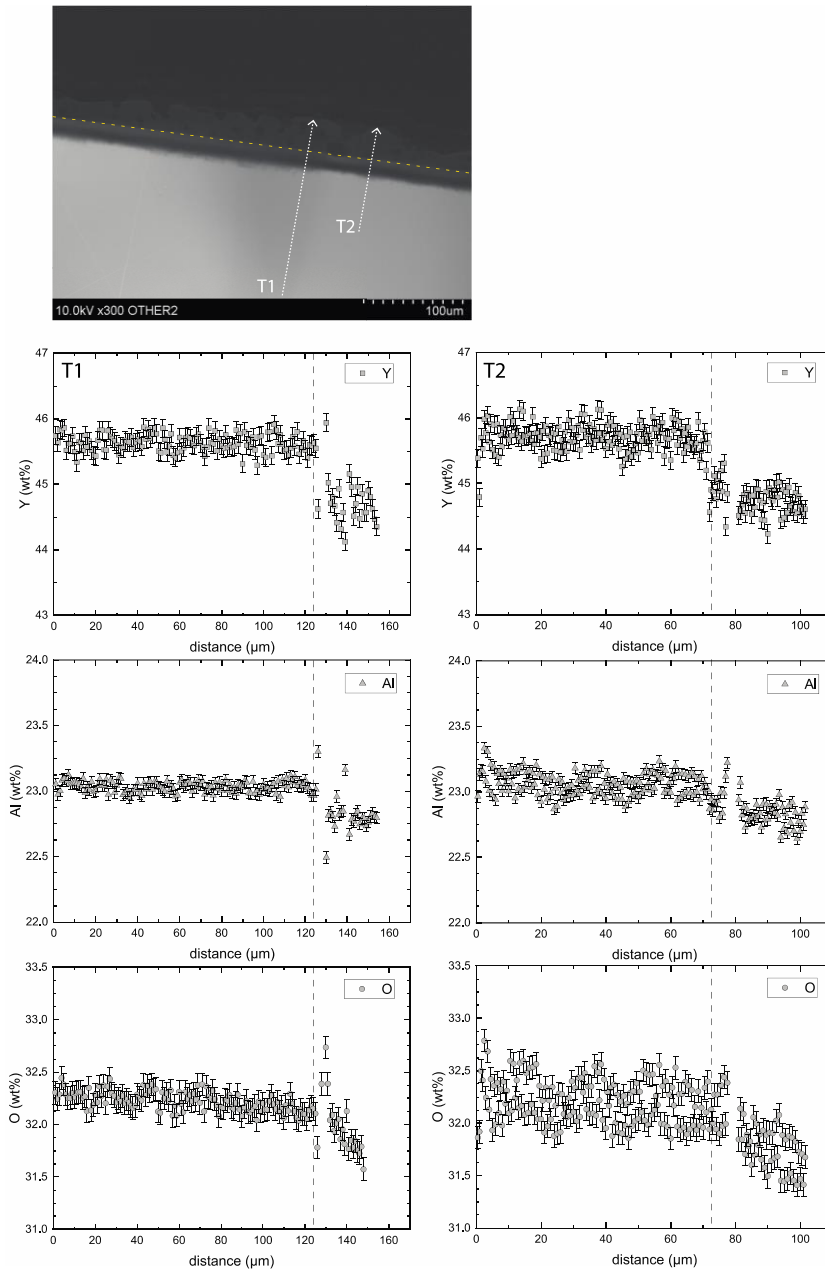


**Figure A1-2.** Quantitative analysis of Y, Al, and O in YAG experimental run products (sample YLPD-1) acquired with EPMA-WDS at 7 kV. Traverses indicated on CL image from YAG substrate through diffusion reacted zone show no obvious change in Y, Al, or O associated with the CL gradient. There is an abrupt change in concentration between the diffusion reacted YAG and buffer overgrowth layer. Quantification of O, and to a lesser extent Al, is affected by secondary fluorescence at the boundary of the sample causing an apparent decrease in concentration.

Garnet cubes ( $\sim 1 \text{ mm}^3$  and  $\sim 3 \times 3 \times 3 \text{ mm}$  for piston-cylinder experiments,  $\sim 2 \times 3 \times 6 \text{ mm}$  for 1-atm experiments) were cut using a 120- $\mu\text{m}$  thick diamond-impregnated wafering blade on a low speed circular saw, and at least one face was polished with diamond paste to a 1- $\mu\text{m}$  finish. Garnet cubes used for HP experiments were polished on their six faces to increase the number of potential analytical surfaces after recovery. Polishing using a colloidal silica-based slurry was attempted once, but did not yield better-polished surfaces.

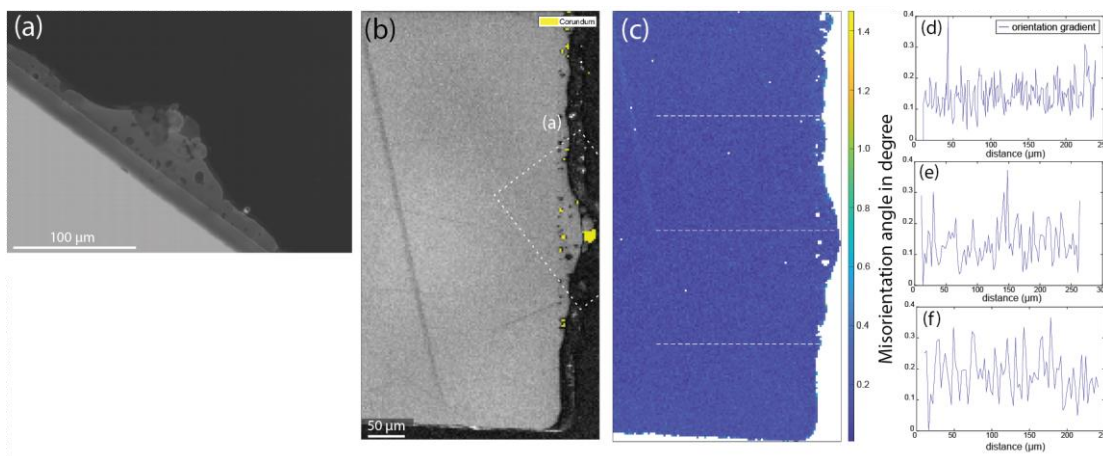


**Figure A1-3.** EBSD analysis of YAG experimental run product (sample YLPD-1). The location of the YAG substrate, diffusion reacted margin, and buffer overgrowth layer are visible in CL (a). EBSD band contrast image shows YAG crystal and encapsulated matrix grains of corundum. A color contoured map of lattice misorientation (c) and three linear traverses (d-f) indicate no crystallographic misorientation across the experimental diffusion zone or synthetic YAG-buffer overgrowth.

### Starting material: powder sources

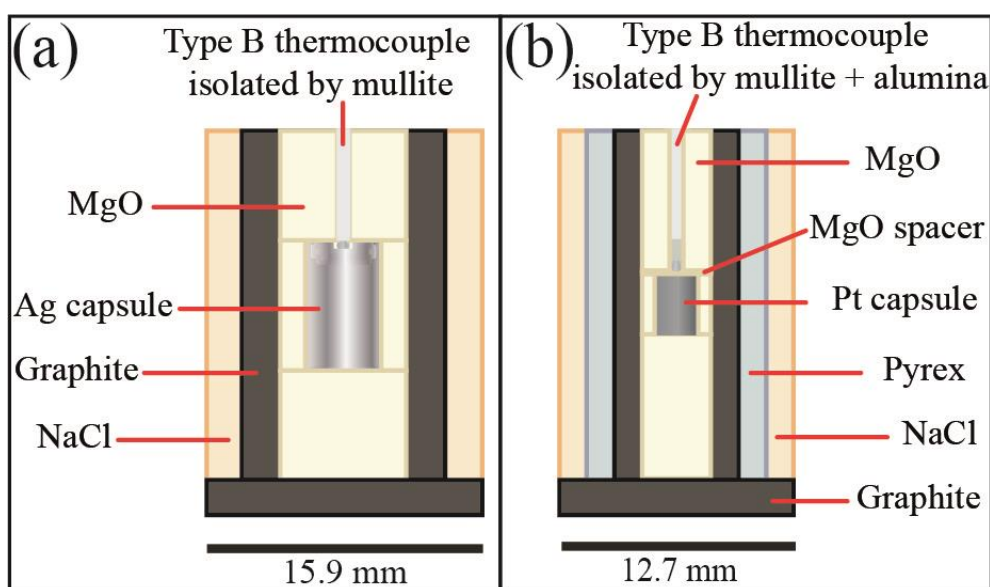
$^{18}\text{O}$ -enriched diffusant source powders for nominally dry experiments at low- and high-pressure were prepared using the sol-gel method, which is superior to simply mixing together powders when working with refractory components. Firstly,  $\text{Y}_2\text{O}_3$  powder and Al metal powder were weighed in proportions to give  $\sim 30 \text{ wt.}\% \text{ Al}_2\text{O}_3$  and  $70 \text{ wt.}\% \text{ Y}_3\text{Al}_5\text{O}_{12}$ . These were then dissolved, separately, in  $\text{HNO}_3$  in Teflon<sup>®</sup> beakers. The solutions were combined, left on a hot

plate to reduce in volume, then a gel was precipitated by the addition of concentrated ammonia. The gel was dried, then the residue was placed into a Pt crucible and held over a Bunsen burner flame until visible fumes were no longer evolved. The crucible was then placed into a box furnace at 1200 °C to remove any remaining volatile components. Aliquots of the resulting powder were then placed into thick-walled, cold-sealed silver capsules (~6.3 mm outer diameter, OD) together with <sup>18</sup>O-enriched H<sub>2</sub>O and annealed in an end-loaded piston-cylinder apparatus at  $T = 975$  °C and  $P = 2.0$  GPa for 48 h. This capsule design was described by Hack and Mavrogenes (2006) and is particularly suited for large-volume hydrothermal experiments because it can be cold-sealed by swaging in a hydraulic press. The fidelity of the experimental design, in terms of retaining water during experiments at equivalent  $P$ - $T$ - $t$  conditions, has been demonstrated previously (e.g. Jollands et al. 2016a; Tollan et al. 2018). After filling and swaging the capsules closed, each capsule was placed into an MgO-graphite-NaCl assembly (Fig. A1-4a). The temperature was monitored and controlled with a type B thermocouple (Pt<sub>70</sub>Rh<sub>30</sub>-Pt<sub>94</sub>Rh<sub>6</sub>) isolated by a two-bore mullite tube (or alumina-tipped mullite for  $T > 1200$  °C runs) and connected to a Eurotherm controller (Fig. A1-4a). A  $P$  of ~0.1 GPa was added before heating; then,  $T$  was increased at 100 °C/min, and  $P$  was increased simultaneously with the aim of approximately following an isochore, according to Hack and Mavrogenes (2006). The pressure was manually adjusted throughout the experiment, as necessary. Experiments were quenched by turning off the power – the temperature on the Eurotherm controller dropped to ~40 °C in a few seconds (e.g., Hermann et al. 2016). The residual pressure was released gradually over ~30 min.

After the HP anneal, the YAG buffer was analyzed by X-ray diffraction in order to confirm the synthesis of YAG plus corundum (Crn), the presence of which means that the yttria and alumina activities are fully buffered (Warshaw and Roy 1959). The <sup>18</sup>O-enriched garnet buffer was then ground to a fine powder under acetone in an agate mortar and used for gas mixing and

HP nominally dry experiments (see below).  $^{18}\text{O}$ -enriched pyrope powder was prepared in a similar way by annealing fine-grained pyrope (Prp-1) and  $^{18}\text{O}$ -enriched  $\text{H}_2\text{O}$  in Ag capsules at  $T = 900\text{ }^\circ\text{C}$  and  $P = 1.0\text{ GPa}$  for 48 h.

Powders not enriched in  $^{18}\text{O}$  were prepared simply by crushing pyrope and grossular to a fine powder, or sintering a pellet of the  $\text{Y}_2\text{O}_3\text{-Al}_2\text{O}_3$  mix prepared using the sol-gel method at  $1400\text{ }^\circ\text{C}$  in air (i.e. instead of hydrothermal sintering with  $^{18}\text{O}$ -enriched  $\text{H}_2\text{O}$ ). These three powders were used for HP experiments under water-present conditions (see below).



**Figure A1-4.** Schematic illustration of experimental assemblies for wet (a) and nominally dry (b) HP experiments.

See text for details.

### Diffusion experiments and run products

**Gas mixing furnace experiments.** Experiments were conducted with YAG crystals, which had been ultrasonically cleaned in ethanol, coated with  $^{18}\text{O}$ -enriched YAG+Crn buffer powder (see above) mixed with polyethylene oxide glue. The experimental charges (i.e., crystal+buffer) were dried overnight in an oven at  $\sim 100\text{ }^\circ\text{C}$ , placed into a platinum holder, and suspended inside

a gas mixing vertical tube furnace. Experiments were performed at 1500 °C and 1600 °C for 168 h and 24 h, respectively (Table 1). The final temperature was reached at a rate of 6 °C/min after ramping up from 600 °C. The furnace was flushed with Ar to limit loss of  $^{18}\text{O}$  from the buffer, which means that the  $f_{\text{O}_2}$  was not buffered, but instead controlled by impurities in the Ar gas. To prevent crystals from breaking, experiments were ended by firstly cooling the furnace down to ~600 °C at a rate of 5 °C/min and then pulling out the charges from the top of the furnace.

Crystals were recovered from 1-atm experiments at 1500 °C and 1600 °C. The  $^{18}\text{O}$  buffer sintered on the surface of the crystal and could not be removed by sonication (Fig. 1a). The crystals were cut orthogonally to the diffusion interface, using a low-speed circular saw as above (Fig. 1b). One of the halves of each crystal was mounted in epoxy, ground with SiC paper (p1200, ~15  $\mu\text{m}$  grit) and polished with diamond paste (3  $\mu\text{m}$  and 1  $\mu\text{m}$ ) to be analyzed in line-scan mode by SIMS (Figs. 1c-e). SEM imaging in cathodoluminescence (CL) mode shows a thin, relatively dark CL band with constant thickness at the interface between the  $^{18}\text{O}$ -YAG+Crn buffer and the YAG cube (Fig. 1e; Table S1, electronic supplement) as well as along all other edges of the crystal not in contact with the  $^{18}\text{O}$ -buffer.

**High-pressure experiments under water-present conditions.** Experiments were conducted using three different garnet compositions (i.e., YAG, Grs-2, and Prp-1). Garnet cubes (1  $\text{mm}^3$ ) were embedded into a matrix made of a fine-grained powder of the same composition plus  $^{18}\text{O}$ -enriched  $\text{H}_2\text{O}$  (Fig. A1-5a). The amount of  $\text{H}_2\text{O}$  added to the capsule was enough to ensure visible water saturation. A sintered YAG+Crn powder was used as the matrix for the YAG experiments (see above). Experiments with YAG, Prp-1, and Grs-2 were performed in end-loaded piston cylinder apparatus at  $T = 900$  °C and  $P = 1.0$  GPa for 14 days. A second experiment under these  $P$ - $T$  conditions was conducted with a larger YAG cube (~3  $\times$  3  $\times$  3 mm) to enable preparation for backward depth-profiling analysis by SIMS. Additional experiments

with YAG and Prp-1 were performed at  $T = 900\text{ }^{\circ}\text{C}$  and  $P = 1.5\text{ GPa}$  for 14 days to investigate the effect of  $P$  on oxygen diffusivity (Table 1).

The experimental setup was similar to that used for the hydrothermal sintering of the source powders. For each experiment with YAG and pyrope, a layer of graphite powder was placed at the bottom of the silver capsule (Fig. A1-5a) to buffer the  $f_{\text{O}_2}$  (based on the buffered C-O-H equilibria; Connolly and Cesare 1993). For each experiment with grossular, the Re-ReO<sub>2</sub> oxygen buffer (Pownceby and O'Neill 1994) was used to produce more oxidizing conditions to stabilize the andradite component. A garnet cube was embedded into fine-grained garnet powder atop the  $f_{\text{O}_2}$  buffer powder, then <sup>18</sup>O-enriched H<sub>2</sub>O was added (Fig. A1-5a).

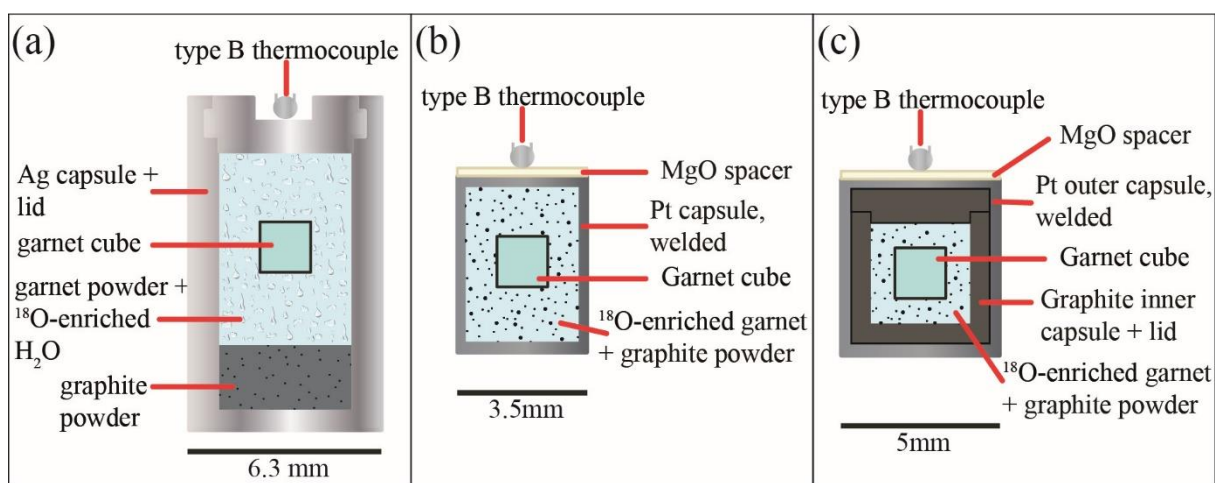


**Figure A1-5.** Schematic illustration of a cold-sealed Ag capsule used for HP experiments under water-present conditions (a), a 3.5 mm Pt capsule (b), and graphite-lined platinum capsules used for nominally anhydrous HP experiments (c). See text for details.

Silver capsules recovered from the HP experiments under water-present conditions were pierced with a 1 mm drill bit to ensure water was still present and under pressure (i.e., no leaks formed during the experiment). The capsules were then opened on each face and crystals were removed, then cleaned ultrasonically to remove residual powder. The YAG crystals showed no

evidence of dissolution, whereas the natural garnets did (Figs. 2a, b). In particular, grossular and pyrope crystals annealed at 1.0 and 1.5 GPa, respectively, were affected by intense dissolution that damaged the original diffusion interface and prevented further analysis. Pyrope annealed at 1.0 GPa (sample PHPW-1, Table 1) was affected by only localized dissolution (Fig. 2b), thus partially preserving the original diffusion interface. The best face of each recovered crystal was mounted in epoxy for forward depth profiling analysis by SIMS (towards the crystal core; Tables 2 and S2, electronic supplement); these were not repolished. The recovered  $3 \times 3 \times 3$  mm YAG crystal was cut in half. One half was prepared and analyzed as above. The second half was ground to a thickness of  $\sim 10$ - $12$   $\mu\text{m}$  and further polished to a final thickness of  $\sim 5$   $\mu\text{m}$ . It was then mounted in an epoxy disc for backward depth profiling analysis by SHRIMP (towards the crystal rim; low to high  $^{18}\text{O}$  with increasing depth) to estimate the extent of edge effects (i.e., the contribution to the apparent diffusion profile arising from secondary ions sputtered from the edge of the crater) with this instrument.

**High-pressure experiments under nominally anhydrous conditions.** This experimental approach was developed to overcome some of the difficulties encountered during the hydrous experiments, mainly dissolution occurring in the presence of water and relatively low melting temperatures of the silver capsule material. Diffusion under nominally anhydrous conditions was thus investigated using garnet cubes embedded into a matrix made of graphite powder and fine-grained powder of YAG+Crn previously enriched in  $^{18}\text{O}$  (see above; Figs. A1-5b, c). Graphite was added with the aim of limiting sintering of the garnet powder onto the cube, as in Van Orman et al. (2001, 2002). The proportions of graphite to garnet powder were always kept constant (i.e., 2:1 ratio by weight). No water was added to these runs.

Experiments with YAG were conducted over the  $T$  range of 1050-1600  $^{\circ}\text{C}$  at  $P = 1.5$  GPa. An additional experiment with YAG was conducted at  $T = 1500$   $^{\circ}\text{C}$  and  $P = 2.5$  GPa to further



**Table A1-2.** Representative major element compositions (wt.%) by EDXA-SEM of natural garnet crystals used for the experiments. Cations are based on 12 oxygens.

<b>Garnet</b>	<b>Grs-2</b>	<b>Grs-2</b>	<b>2SD</b>	<b>Prp-1</b>	<b>Prp-1</b>	<b>Prp-1</b>	<b>2SD</b>
<b>Analysis n.</b>	<b>1</b>	<b>2</b>	<b>Grs-2</b>	<b>1</b>	<b>2</b>	<b>3</b>	<b>Prp-1</b>
SiO <sub>2</sub>	39,4	39,6	0,28	41,3	41,9	41,1	0,83
Al <sub>2</sub> O <sub>3</sub>	22,7	22,2	0,71	23,7	23,9	23,1	0,83
FeO	2,2	2,9	0,99	15,4	14,6	15,7	1,14
MnO	0,1	0,3	0,28	0,4	0,3	0,5	0,20
MgO	< 0,1	0,1	0,10	18,7	18,7	19	0,35
CaO	35,6	34,9	0,99	0,6	0,7	0,7	0,12
<b>Total</b>	<b>100</b>	<b>100</b>	<b>&lt;0,01</b>	<b>100</b>	<b>100</b>	<b>100</b>	<b>&lt;0,01</b>
Si	2,97	2,99	0,028	2,98	3,02	2,97	0,053
Al	2,01	1,97	0,057	2,01	2,02	1,96	0,064
Fe <sup>3+</sup> (calculated)	0,05	0,05	<0,001	0,03	0	0,11	0,114
Fe <sup>2+</sup> (calculated)	0,09	0,14	0,071	0,9	0,88	0,84	0,061
Mn	0,01	0,02	0,014	0,02	0,02	0,03	0,012
Mg	0	0,01	0,014	2,01	2,01	2,04	0,035
Ca	2,87	2,82	0,071	0,05	0,05	0,05	<0,001
<b>Total of Cations</b>	<b>8</b>	<b>8</b>	<b>&lt;0,001</b>	<b>8</b>	<b>8</b>	<b>8</b>	<b>&lt;0,001</b>
Almandine	0,03	0,05	0,03	0,3	0,3	0,28	0,02
Pyrope	< 0,01	< 0,01	<0,01	0,67	0,68	0,69	0,02
Grossular	0,94	0,92	0,03	0,02	0,02	0,02	<0,01
Spessartine	< 0,01	0,01	0,01	0,01	0,01	0,01	<0,01
Andradite	0,02	0,02	<0,01	< 0,01	< 0,01	< 0,01	<0,01